ADDITIONAL THEORY OF THE DOUBLE X-RAY SPECTROMETER

By Roy C. Spencer
Columbia University

(Received June 22, 1931)

Abstract

It is shown that an x-ray which comes from a point source and is reflected from a fixed and a moving crystal must pass through a focal point fixed in space and also through a second focal point moving with the crystal. These focal points are the best positions for the location of an ionization chamber window or slit. A universal type of crystal mounting is described which permits the study of wave-lengths from 0 to 5A without readjustment of the crystals. This style of spectrometer can also be used to measure absolute reflection angles. By using a thin glass window in the x-ray tube and a hydrogen atmosphere around the crystals, wave-lengths of 5A may be studied. Graphical methods have been developed which show the effect of the crystal curve and the vertical height of the slits on the shape of the wave-length curve. This method can also be used in other types of spectroscopy to study the effect of the spectrometer on the curve.

Part 1. Geometry and Design

THE double x-ray spectrometer was used by Davis and Stempel[1] with the crystals in the parallel position to study the reflecting properties of the crystals. The two-crystal spectrometer has high resolving power when the crystals are used in the antiparallel position. The development of this type of spectrometer was made simultaneously by Bergen Davis and Purks,[2] Ehrenberg and Mark[3] and Ehrenberg and Susich[4] who applied it to the study of the natural breadth of spectral lines. This type of spectrometer has been described in detail by Williams and Allison.[5] M. M. Schwarzchild[6] has given a mathematical theory of the instrument. The design has been modified by Richtmyer[7] and by DuMond and Hoyt.[8]

The following discusses some further points of geometry of the double x-ray spectrometer in which the source and one of the crystals remains fixed, and describes a "universal" type of mounting which is simpler and covers a wider range of angles than the previous types. This type of mounting has been used for over a year by the author

The reflection of x-rays from crystals may be treated exactly as the reflection of light from plane mirrors except that there is the added condition

$$n\lambda = 2d \sin \theta \qquad (1)$$

[1] Davis and Stempel, Phys. Rev. **17,** 608 (1921).
[2] Davis and Purks, Proc. Nat. Acad. Sci. **13,** 419 (1927).
[3] Ehrenberg and Mark, Zeits. f. Physik **42,** 807 (1927).
[4] Ehrenberg and Susich, Zeits. f. Physik **42,** 823 (1927).
[5] Williams and Allison, J.O.S.A. and R.S.I. **18,** 473 (1929).
[6] M. M. Schwarzchild, Phys. Rev. **32,** 162 (1928).
[7] Richtmyer, Barnes and Ramberg, Phys. Rev. **35,** 1428A (1930).
[8] DuMond and Hoyt, Phys. Rev. **36,** 1702 (1930).

where n is the order of reflection and d is the grating constant of the crystal. The ray $SABF$ is shown in Fig. 1 reflected from crystal A at second order and from crystal B at third order. In general, the orders of reflection will be n_1

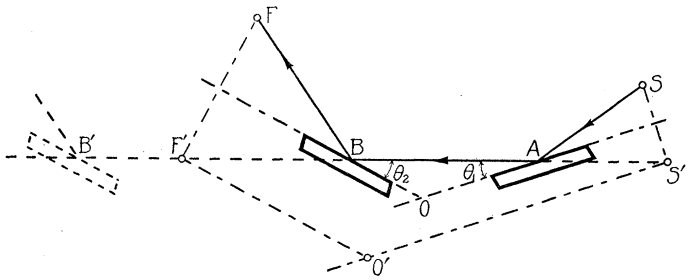

Fig.1. Path of an x-ray reflected from two crystals. S and S' are the real and virtual sources. A and B are the points of incidence at the crystals. If the plane containing crystal B and the points F and F' is rotated about O' as an axis, then F' becomes a virtual focus and F a real focus for any ray from S which is reflected from both crystals.

and n_2. The wave-length may be eliminated from two equations of the type of Eq. (1) resulting in

$$n_1/n_2 = \sin\theta_1/\sin\theta_2 \tag{2}$$

O is the intersection of the two crystal planes. An application of the sine law to triangle OAB shows that

$$OB/OA = \sin\theta_1/\sin\theta_2. \tag{3}$$

From Eqs. (2) and (3)

$$OB/OA = n_1/n_2. \tag{4}$$

For various wave-lengths the position of the source S may be so adjusted that the ray is incident at the same point A on crystal A. If crystal B is rotated about O as an axis, OA is then constant and OB must also be constant by Eq. (4). The ray will then be incident at the same point B on crystal B. The points A and B are conjugate foci. This arrangement might be called a "universal" spectrometer, for any wave-length from 0 to $2d/n$ may be studied without readjustment of the crystals.

When the source is fixed in position, the points of incidence A and B are not fixed in the crystals. In Fig. 1 S' is the image of the source S in the plane of crystal A. Rays such as $S'AB$ radiate from S' in all directions. For any direction making an angle θ with the crystal plane, only one wave-length will be reflected according to Eq. (1). The other wave-lengths will be absorbed in the crystal. In order to simplify the theory, the axis of rotation of crystal B has been moved to O' which is any point along a line through S' parallel to crystal A. $O'F'$ is drawn parallel to crystal B and intersects $S'B$ in F'. F is a point such that F' is its image. From similar triangles and Eq. (4).

$$O'F'/O'S' = n_1/n_2. \tag{5}$$

The points S' and F' are imaginary conjugate foci by the same reasoning that was applied to the points A and B. The points S and F are real conjugate foci since any ray coming from S must pass through F.

A mechanical model may easily be made in which a plane containing F, F' and crystal B rotates about O' with respect to the fixed plane containing S, S' and crystal A. A string held taut between S' and F' gives the actual path of the ray between the crystals. The points A and B are seen to slide to the outer portions of the crystals as the angles of reflection increase. If S represents the source of the x-rays, then F might represent the small window of an ionization chamber. This arrangement would eliminate any movement of the beam across the chamber window and would allow the use of a window as narrow as the source. Slits placed elsewhere along the beam would have to be wider.

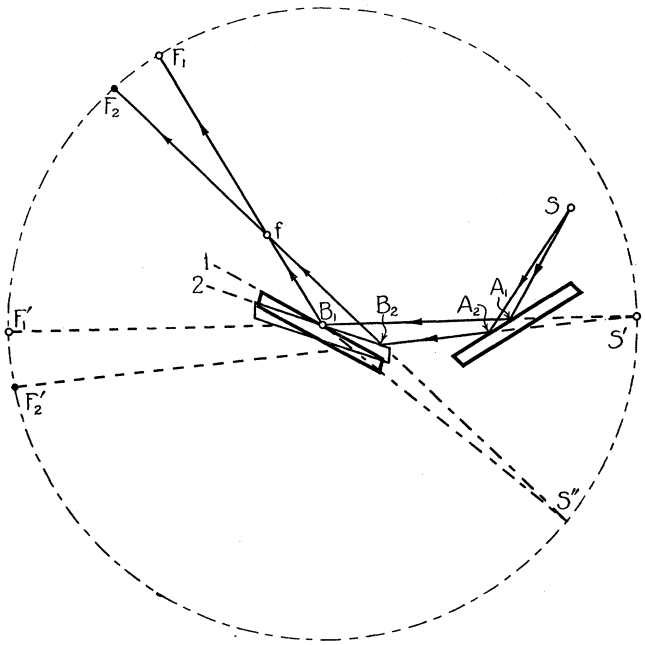

Fig. 2. Usual type of double x-ray mounting with axis at center of crystal B at B_1. The orders of reflection are the same at each crystal. Two positions of crystal B are shown. The corresponding rays intersect at f which is a focus fixed in space in contrast to F which is a focus moving with the crystal. The distance B_1f is approximately one third of B_1S'.

An interesting arrangement is the one in which crystal B is beyond F' at B'. F and F' then coincide and the real focus is between the two crystals. Should the axis of rotation be placed elsewhere, the focal point may degenerate into a caustic curve.

The discussion up to now has assumed a different order of reflection at each crystal. The usual practice is to have both orders of reflection the same. In this case OA equals OB which allows the axis O' to lie anywhere in space. Two such arrangements will be described.

The first is the usual type of mounting in which the axis of rotation is at B_1, the center of the second crystal. (See Fig. 2.) The notation is the same as in Fig. 1. If the plane containing F_1, F_1' and crystal B is rotated through an

angle $2\Delta\theta$ counter clockwise, then F_1 and F_1' assume the new positions F_2 and F_2'. The line $S'F_2'$ now marks off A_2 and B_2 as the new points of incidence and the reflected ray B_2F_2 intersects the former ray B_1F_1 in f which will be proved to be a real focal point "fixed in space." Let the triangle B_1B_2S' be imaged in the crystal plane B_1B_2. Then S'' is the image of S' and $S''B_2f$ is a straight line. An application of the sine law to triangle B_1fS'' gives

$$\frac{B_1f}{\sin\Delta\theta}=\frac{B_1S''}{\sin 3\Delta\theta}. \tag{6}$$

Now $B_1S''=B_1A_1+A_1S=L$, the distance of the source from the axis B_1. From Eq. (6)

$$B_1f=\frac{\sin\Delta\theta}{\sin 3\Delta\theta}L=\frac{L}{3}\text{ (approx.)} \tag{7}$$

when $\Delta\theta$ is not more than a few degrees. This proves that all rays from S cross at a point f, fixed in space such that the distance from the axis to f is approximately one-third the optical distance from the source to the axis.

The second type of mounting is one used by the author (see Fig. 3). The axis of rotation O' is symmetrically placed with respect to the two crystals.

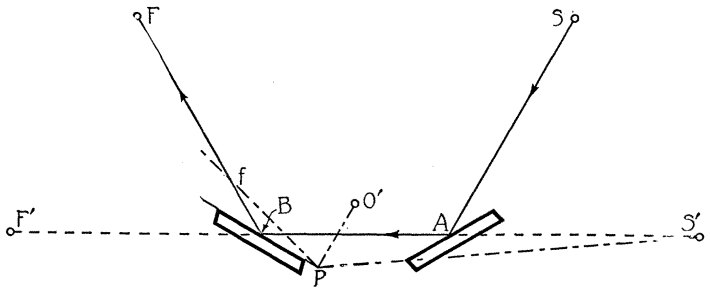

Fig. 3. Universal type of double x-ray mounting with axis at any point O' which is symmetrical to the two crystals. The two crystals will remain symmetrical even though crystal B is rotated through large angles. This makes possible the study of x-rays incident on the crystals at any angle. The instantaneous axis of rotation of crystal B is at P. The focus fixed in space is at f.

Although crystal B rotates about O', the instantaneous axis of rotation in its own plane is at P, the foot of the perpendicular from O'. Using Eq. (7) the distance Pf is approximately one third of $S'P$. The advantage of the universal type of mounting is as follows. The beam may at all times be reflected from the same portions of both crystals no matter how large the angle, by simply moving the source sidewise. In the usual type, however, if the beam is reflected from the same portion of one crystal, it will move off of the other crystal.

The principle of reversibility can be applied to any double crystal arrangement. The ionization chamber window can be placed at S. The source can remain fixed at f or can move with the crystal when placed at F.

Measurement of Large Angles by Means of the Universal Type of Mounting

The universal type of mounting as just described can measure all angles from 0 to as near 90° as desired.

In order to determine the reflection angle at say first order, it is necessary to measure the difference in angle ϕ between first and second order. The difference in circle positions is, of course 2ϕ. A different effective grating constant must be used for each order[9] to correct for refraction. From Eq. (1)

$$\lambda = 2d_1 \sin\theta_1 = d_2 \sin\theta_2 \tag{8}$$

But

$$\sin\theta_2 = \sin(\theta_1 + \phi) \tag{9}$$

Substituting (9) in (8)

$$\tan\theta_1 = \frac{\sin\phi}{(2d_1/d_2) - \cos\phi} \tag{10}$$

Eq. (10) gives the absolute angle θ_1 at which first order reflection occurs. Subtracting $2\theta_1$ from the position on the circle at first order gives the zero of the circle, so that measurements of 2θ for any other x-ray line may be read directly.

The usual type of double x-ray spectrometer can also be used to measure reflection angles by taking curves in the parallel and antiparallel positions. The second crystal is turned through $180°-2\theta$.

In another paper a method is given by which x-rays up to the limit of the calcite crystal can be studied using the double x-ray spectrometer.

Part II. Distortion of X-ray Lines by Vertical Divergence and Crystal Width

Shape of monochromatic line due to vertical divergence

The axis of the spectrometer and the crystal planes were made vertical by methods which will be given in a later paper. Eq. (19) of Schwarzchild[6] could then be simplified to

$$\delta = \psi^2 \tan\theta = \psi^2/C^2 \tag{11}$$

where ψ is the angle between the ray and the horizontal plane, called the angle of vertical divergence, and δ is the angular deviation of the position of the second crystal from the position it would have if ψ were zero. The energy reflected from the second crystal is some function $I(\psi)$ which depends on the energy distribution across the target and on the slits limiting the vertical angle.

$$I(\psi) = \frac{dE}{d\psi}. \tag{12}$$

Since $I(\psi)d\psi = I(\delta)d\delta$ the distribution of energy with δ may be found by a change of variable using Eq. (11)

[9] Siegbahn, Spectroscopy of X-rays, p. 21.

$$I(\delta) = \frac{dE}{d\delta} = \frac{CI(C\delta^{1/2})}{2\delta^{1/2}} \tag{13}$$

The simplest case is that of a beam diverging from a point source and limited by a slit of height H, level with the source, but at a distance L from it. $I(\psi)$ is a constant K for $|\psi| < H/2L$

$$I(\delta) = \frac{CK}{\delta^{1/2}} \cdot \tag{14}$$

The curve of Eq. (14) is shown in Fig. 4. This differs from the curve given by Schwarzchild[6] but the equation is in agreement with that given by DuMond

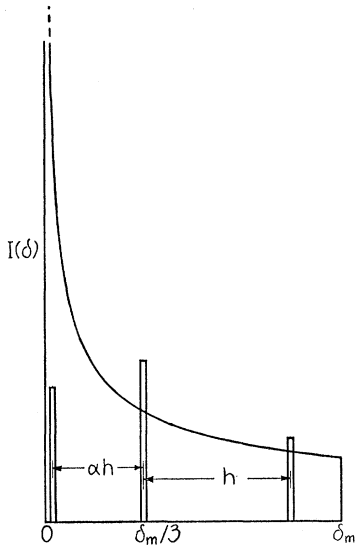

Fig. 4. Distortion of monochromatic line by vertical divergence for the case of a beam diverging from a point source and limited by a slit of height H distant L from the source. The maximum angle of vertical divergence ψ_m is $H/2L$. The maximum deviation δ_m in the position of crystal B is $\psi_m^2 \tan\theta$. The center of gravity of the curve is shifted $\delta_m/3$ from the position of the monochromatic line at O. The three pillars give the position and relative intensity of three components whose first four moments are equal respectively to the first four moments of the curve.

and Hoyt[8] for the same conditions (see their Fig. 3). The two axes of their figure have apparently been interchanged since their curve approximates more closely $K/2\delta^2$.

The next simplest case is that of a beam diverging from a broad uniform source and limited by two slits of equal height, H, separated by distance L. The maximum value of ψ is H/L. A curve of the intensity with ψ is an isosceles triangle

$$I(\psi) = K'(\psi_m - |\psi|)$$

$$I(\delta) = \frac{K'\delta_m^{1/2}}{\tan\theta}\left(\frac{1}{\delta^{1/2}} - \frac{1}{\delta_m^{1/2}}\right) \tag{15}$$

where δ_m is the maximum value of δ. The shape of this curve (see Fig. 5) is the same as Fig. 4 except that the δ-axis has been raised. The curve of intensity with Ψ caused by two unequal slits is an isoscles trapezoid.[10] This is the difference of two triangles. Hence the curve of intensity with δ is the difference of two curves of the type of Eq. (15).

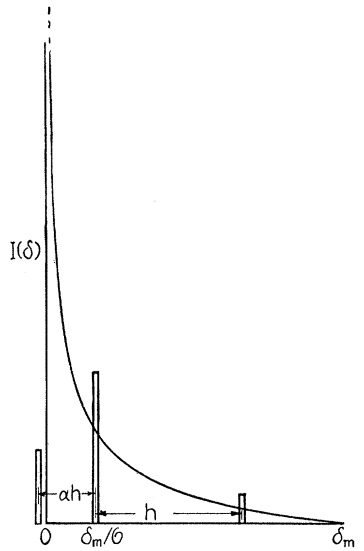

Fig. 5. Same as Fig. 4 but for the case of a beam diverging from a broad uniform source and limited by two equal slits of height H distant L from each other. $\psi_m = H/L$. The center of gravity is shifted $\delta_m/6$ from the origin.

As pointed out by DuMond and Hoyt the area of Fig. 4 is finite, although the intensity at the origin is infinite. The centers of gravity of Figs. 4 and 5 are distant $\delta_m/3$ and $\delta_m/6$ respectively from the origin. This is very important as it shifts the center of gravity of any x-ray line by the same amount. The equivalent shift in wave-length may be obtained by differentiating Eq. (1). Hence

for Fig. 4

$$\frac{\Delta\lambda}{\lambda} = \frac{H^2}{12L^2} \tag{16}$$

for Fig. 5

$$\frac{\Delta\lambda}{\lambda} = \frac{H^2}{6L^2}. \tag{17}$$

The fractional change of wave-length is, therefore, independent of angle. For precise wave-length measurements this should be made small by narrowing the slits or making L large. If the intensity across the target were uniform (which never occurs), the shift could be calculated.

In photographic measurements the position of the line may be measured

[10] Richtmyer, Phys. Rev. **26**, 724 (1925).

at the center. However, the central point receives rays from various parts of the target of height H. If L is the distance of the photographic plate, then Eq. (16) gives the correction.

Methods of analyzing spectrometer curves

The author first became interested in this subject while associated with F. K. Richtmyer[10] in a study of the single crystal spectrometer. The effect of any spectrometer is to transform a monochromatic line of infinitesimal width into a curve $F(\theta)$. In general it will transform a curve $\phi(\theta)$ into a curve $G(\theta)$.

Ehrenberg and Mark[3] and Ehrenberg and Susich[4] were the first to attempt to correct for the width of the crystal. They assumed that all three curves were Gaussian in shape in which case the relation of the widths at half maximum is

$$W_G^2 = W_\phi^2 + W_F^2. \tag{18}$$

Allison and Williams[11] used the above formula to correct for the crystal width W_F. The author believes that their method of correcting for vertical divergence, however, is in error. In the first place they assume that the width at half maximum of the curve $I(\delta)$ is related to the width at half maximum of $I(\psi)$ by Eq. (11). This is incorrect since the width at half maximum of $I(\delta)$ is zero. In the second place they subtract this width from the measured width of the line, whereas Eq. (18) would have been more correct. Valasek[12] has also subtracted his crystal and slit widths from the measured width of the line. In practice the wave-length and crystal curves are not Gaussian in shape, so it is necessary to develop the theory more carefully.

It is observed that the intensity at any point of $G(\theta)$ is the sum of contributions of the original curve on either side. If the areas under $\phi(\theta)$ and $F(\theta)$ are each unity, the equation for $G(\theta)$ can be put in either of the following forms.

$$G(\theta) = \int_{-\infty}^{\infty} \phi(\theta - \beta)F(\beta)d\beta \tag{19}$$

or

$$G(\theta) = \int_{-\infty}^{\infty} \phi(\beta)F(\theta - \beta)d\beta. \tag{20}$$

Eqs. (19) and (20) are integral equations. A solution for $\phi(\theta)$ is impractical to use, so we will assume $\phi(\theta)$ and study the quantity $G(\theta)-\phi(\theta)$ by which $\phi(\theta)$ is elevated at any point. $\phi(\theta)$ is usually wider and smoother than $F(\theta)$ and so in Eq. (19) can be expanded by Taylor's theorem in powers of β

$$G(\theta) = \phi(\theta) - \frac{\phi'(\theta)}{1}\mu_1 + \frac{\phi''(\theta)}{2!}\mu_2 - \frac{\phi'''(\theta)}{3!}\mu_3 + \cdots \tag{21}$$

where the nth moment of $F(\beta)$ is

$$\mu_n = \int_{-\infty}^{\infty} \beta^n F(\beta)d\beta.$$

If the center of gravity of $F(\beta)$ is taken as the origin, then $\mu_1 = 0$.

[11] Allison and Williams, Phys. Rev. **35**, 1476 (1930).

[12] Valasek, Phys. Rev. **36**, 1523 (1930).

Equivalent triplet

It will be shown later that any curve $F(\beta)$ may be replaced by a triplet, so arranged that the first four moments of the triplet are equal respectively to the first four moments of $F(\beta)$. See Figs. 4 and 5. The central component is placed at the center of gravity. The other two components are placed at distances h and $-\alpha h$ from the central component and comprise a fraction β of the total weight. The fraction β is not to be confused with the β of $F(\beta)$. The nth moment is given by

$$\mu_n(1 + \alpha) = \beta h^n(\alpha \pm \alpha^n) \tag{22}$$

the $-$ sign being used when n is even. This triplet can now be used in a simple graphical solution which corrects for the first five terms of Eq. (21).

Fig. 6 shows three vertical lines separated by the same distances as were

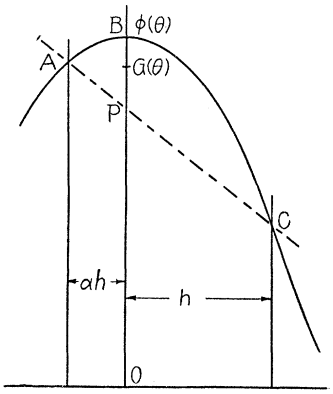

Fig. 6. Graphical solution for the effect of the vertical divergence in Fig. 5 on the shape of an x-ray line $\phi(\theta)$. Three vertical lines whose separations are those of the triplet solution cut $\phi(\theta)$ in points A, B and C. The line AC cuts the central line at P. The value of $\phi(\theta)$ at B is lowered to $G(\theta)$ such that $G(\theta) - B = \beta\overline{BP}$. The value of β is given in Table I. There is also a lateral displacement equal to the position of the center of gravity of Fig. 5. For the inverse solution see text.

the triplet components, which cut the curve $\phi(\theta)$ in $\phi(\theta-\alpha h)$, $\phi(\theta)$ and $\phi(\theta+h)$ indicated by points A, B and C. The chord AC cuts OB in P, the position being determined by

$$(1 + \alpha)P = \phi(\theta - \alpha h) + \alpha\phi(\theta + h)$$

$G(\theta)$ is defined as a point such that

$$G(\theta) - \phi(\theta) = \beta\overline{BP}$$

β is a fraction less than 1. If $F(\theta)$ is expanded in a Taylor's series, then $G(\theta)$ will reduce to the form of Eq. (21) in which μ_n is given by Eq. (22). In the case that $\beta = 1$, the triplet reduces to a doublet in which the ratio of intensity of the two components is α. The conditions for the equivalent triplet by use of Eq. (22) are

$$\mu_1 = 0 \tag{23}$$

$$\mu_2 = h^2\alpha\beta \tag{24}$$

$$\mu_3 = h^3\alpha\beta(1 - \alpha) \tag{25}$$

$$\mu_4 = h^4\alpha\beta(1 - \alpha + \alpha^2). \tag{26}$$

Equations derived from these are

$$\frac{(1 - \alpha)^2}{(1 - \alpha + \alpha^2)} = \frac{\mu_3^2}{\mu_2\mu_4} \tag{27}$$

$$h^2 = (1 - \alpha + \alpha^2)\frac{\mu_4}{\mu_2} \tag{28}$$

$$\frac{1}{\beta} = \frac{h^2\alpha}{\mu_2} = \alpha(1 - \alpha + \alpha^2)\frac{\mu_4}{\mu_2^2} \tag{29}$$

$$h(1 - \alpha) = \frac{\mu_3}{\mu_2}. \tag{30}$$

The value of α was found from Eq. (27) which is a quadratic in α. With this value h and β were obtained from Eqs. (28) and (29). A numerical check was made by substituting in Eq. (30) or Eq. (25).

In the case $F(\beta)$ is symmetrical $\mu_3 = 0$ and α is unity by Eq. (27). From Eqs. (28) and (29)

$$h^2 = \frac{\mu_4}{\mu_2} \tag{31}$$

$$\frac{1}{\beta} = \frac{\mu_4}{\mu_2^2}. \tag{32}$$

The ratio μ_4/μ_2^2 is what is known in statistical theory as the "flatness." The flatness of a Gaussian curve is 3.

TABLE I. *Moments and equivalent triplets of various curves.*

Type	$\frac{\mu_1}{d}$	$\frac{\mu_2}{d^2}$	$\frac{\mu_3}{d^3}$	$\frac{\mu_4}{d^4}$	$\frac{\mu_3^2}{\mu_2\mu_4}$	$\frac{\mu_4}{\mu_2^2}$	α	$\frac{h}{d}$	β
I	0	0.333333	0	0.200000	0	0.1250	1	0.7746	0.5556
II	0	0.166667	0	0.066667	0	2.4000	1	0.6325	0.4167
III	0	0.721348	0	1.561029	0	3.0000	1	1.4711	0.3333
IV	0	0.088889	0.016931	0.016931	0.19047	2.1429	0.6185	0.4993	0.5763
V	0	0.038889	0.011640	0.007209	0.48333	4.7668	0.3934	0.4934	0.4060

Type I Rectangle, width $2d$.
Type II Isosceles triangle, maximum width $2d$.
Type III Gaussian curve, half maximum width $2d$.
Type IV and V See Figs. 4 and 5, Moments taken about center of gravity. $\delta_m = d$.

Types I or II are found in optical and x-ray spectrometers in which the angular width of the beam is restricted in the horizontal plane by slits, also in densitometer curves. The grouping of statistical data into equal intervals is another example of type I.

Types IV and V are found in spectroscopic apparatus in which the energy distribution of the beam in the vertical plane is of type I or II. Types IV and V are also found in the Dempster mass spectrograph.

The moments of most of the curves in Table I were easily calculated. However, the moments of types IV and V about the center of gravity were more difficult. They were obtained by

$$\mu_n = \int_{-\infty}^{\infty} F(\beta)(\beta - \beta_0)^n d\beta \tag{33}$$

where β_0 is the center of gravity. An easier method would have been to use the following formulae to obtain the moments directly from the moments about the origin, which are indicated by primes.

$$\begin{aligned} \mu_1 &= 0 \\ \mu_2 &= \mu_2' - \mu_1'^2 \\ \mu_3 &= \mu_3' - 3\mu_1'\mu_2' + 2\mu_1'^3 \\ \mu_4 &= \mu_4' - 4\mu_1'\mu_3' + 6\mu_1'^2\mu_2' - 3\mu_1'^4. \end{aligned} \tag{34}$$

The solution of the constants h and β in the case of the crystal curve was arbitrary. Some energy was detected at a distance of 20 times the half width at half maximum. A base line was drawn at this point. The value of h was twelve times the half width at half maximum. β was 0.05 compared with one third for a Gaussian curve. This solution could not be applied since h was greater than the width of $\phi(\theta)$ and the series in Eq. (21) would not converge rapidly enough. The next method was to resolve the crystal curve $F(\theta)$ into the sum of two curves $F_1(\theta)+F_2(\theta)$ which consisted of the narrow part and the broad base. $F_1(\theta)$ gave a reasonable solution. The broad base $F_2(\theta)$ was broader than $\phi(\theta)$ at half maximum. This meant that it was but slightly smoothed over by $\phi(\theta)$ and could be added directly to the solution $G_1(\theta)$ to give $G(\theta)$.

The combined effect of vertical divergence and crystal width on the shape of x-ray lines.

If the curve $G(\theta)$ given by Eq. (19) is smoothed over by a second factor $F_2(\theta)$ into a curve $H(\theta)$, it can be shown by a double Taylor's series expansion that $H(\theta)$ is of the same form as Eq. (21) except that the single moment, say μ_4, is replaced by the following group of moments and cross moments. The primed moments are those of $F_2(\theta)$.

$$\mu_4 + 4\mu_3\mu_1' + 6\mu_2\mu_2' + 4\mu_1\mu_3' + \mu_4'. \tag{35}$$

Since the first moments are zero there remains

$$\mu_4 + 6\mu_2\mu_2' + \mu_4'. \tag{36}$$

For the lower moments the cross moments vanish. Therefore, approximately the depression of the curve $\phi(\theta)$ due to two or more instrumental factors is equal to the sum of the depressions due to each factor.

In the case in which all the curves are Gaussian in shape, the change in width at half maximum is also approximately equal to the sum of the changes

due to each effect taken separately, except for a cross product in the fourth order.

$$W_H = (W_\phi^2 + W_1^2 + W_2^2)^{1/2}$$

$$W_H = W_\phi + \frac{(W_1^2 + W_2^2)}{2W_\phi} - \frac{(W_1^4 + 2W_1^2W_2^2 + W_2^4)}{8W_\phi^3} + \cdots$$

Method of solving for the original curve

If the graphical solution were applied to the original curve $\phi(\theta)$, it should give the experimental curve $G(\theta)$. If it is applied to the experimental curve $G(\theta)$, it gives a new curve $H(\theta)$. With Eq. (36) $H(\theta)$ may be written as

$$H(\theta) = G(\theta) + [G(\theta) - \phi(\theta)] + \phi^{IV}(\theta)\mu_2^2/4$$

whence

$$\phi(\theta) = G(\theta) + [G(\theta) - H(\theta)] + \phi^{IV}\mu_2^2/4$$

In the last term $\phi^{IV}(\theta)$ may be replaced by $G^{IV}(\theta)$. The interpretation is simple. The depression, say at the peak, found by the graphical method is $G(\theta) - H(\theta)$. This is added directly to the experimental curve $G(\theta)$ and gives a fair approximation to the original curve $\phi(\theta)$ neglecting fourth order terms. If to this is also added the remaining term, then the fourth order terms are accounted for.

This last term was neglected in all calculations made by the author. The precision of the electrometer measurements did not warrant the extra term.

An attempt was made to modify the constants of the graphical solution so as to eliminate the last term. This was impossible as the value of h became imaginary.

Application of theory to x-ray lines

The effect of vertical divergence in shifting the center of gravity of a line has already been fully discussed. In order to calculate the effect of vertical divergence or crystal width on the width of an x-ray line the depression at the peak of the x-ray line was first estimated graphically by drawing in the three vertical lines described above, allowing the central line to pass through the vertex. See Fig. 6. Half the depression at the peak was the depression of the half maximum height. The graphical solution was then applied to each side at half maximum to find the elevation of the curve. This resulted in an additional broadening.

It is interesting to note that the broadening due to the crystal increases with the flatness of the crystal curve and with the sharpness at the peak of the x-ray line. For these reasons the correction in any actual case is larger than that given by Eq. (18).